Published in final edited form as:
IEEE Trans Ultrason Ferroelectr Freq Control. 2009 December ; 56(12): 2760–2763. doi:10.1109/TUFFC.2009.1367.

Design and Fabrication of PIN-PMN-PT Single-Crystal High-Frequency Ultrasound Transducers

Ping Sun,
School of Physical Science and Technology Wuhan University, Wuhan, China, NIH Resource Center on Medical Ultrasonic Transducer Technology, Department of Biomedical Engineering, University of Southern California, Los Angeles, CA

Qifa Zhou,
NIH Resource Center on Medical Ultrasonic Transducer Technology, Department of Biomedical Engineering, University of Southern California, Los Angeles, CA

Benpeng Zhu,
NIH Resource Center on Medical Ultrasonic Transducer Technology, Department of Biomedical Engineering, University of Southern California, Los Angeles, CA

Dawei Wu,
NIH Resource Center on Medical Ultrasonic Transducer Technology, Department of Biomedical Engineering, University of Southern California, Los Angeles, CA

Changhong Hu,
NIH Resource Center on Medical Ultrasonic Transducer Technology, Department of Biomedical Engineering, University of Southern California, Los Angeles, CA

Jonathan M. Cannata,
NIH Resource Center on Medical Ultrasonic Transducer Technology, Department of Biomedical Engineering, University of Southern California, Los Angeles, CA

Jin Tian,
Materials Corp., Bolingbrook, IL

Pengdi Han,
Materials Corp., Bolingbrook, IL

Gaofeng Wang, and
School of Physical Science and Technology Wuhan University, Wuhan, China

K. Kirk Shung
NIH Resource Center on Medical Ultrasonic Transducer Technology, Department of Biomedical Engineering, University of Southern California, Los Angeles, CA

Ping Sun: pingsun@usc.edu

Abstract

High-frequency PIN-PMN-PT single crystal ultrasound transducers at center frequencies of 35 MHz and 60 MHz were successfully fabricated using lead indium niobate-lead magnesium niobate-lead titanate (0.23PIN-0.5PMN-0.27PT) single crystal. The new PIN-PMN-PT single crystal has higher coercivity (6.0 kV/cm) and higher Curie temperature (160°C) than PMN-PT crystal. Experimental results showed that the PIN-PMN-PT transducers have similar performance but better thermal stability compared with the PMN-PT transducers.

I. Introduction

High-Frequency (>20 MHz) ultrasound transducers have been extensively used in dermatology, ophthalmology, small animal imaging, and intravascular applications [1], [2]. In an ultrasound transducer, the piezoelectric layers is the most crucial component because it is utilized as the active element to transform the electric input into a mechanical wave propagating into the targets to be imaged and vice versa. Among a wide range of piezoelectric materials, relaxor-based PZN-PT and PMN-PT, which have extremely high transmission constant (d_{33} = 2000 to 3000 pC/N) and electromechanical coupling coefficient (k_{33} = 85 to 95%), exhibit excellent piezoelectric performances [3], [4] and have been used in advanced medical ultrasound imaging systems [5]. However, for binary PMN-PT crystals, the coercive field (2.5 kV/cm) has been found to be low, which is undesirable for applications where the excitation signal is high. Moreover the low Curie temperature (T_C ~130°C) of the PMN-PT crystals leads to deteriorating transducer performance at an elevated temperature. Thus, the development of new single crystals with higher coercivity and high T_C with a superior thermal stability for ultrasound transducer applications has generated much interest recently. The addition of lead indium niobate PIN to PMN–PT crystals has been shown to increase the transition temperature [6], [7]. The ternary PIN–PMN–PT single crystals, with high coercivity (6.0 kV/cm) and high Curie temperature (160°C), yield better thermal stability for performance of transducers. Therefore, it is considered a promising material for applications in high-frequency pulse-wave Doppler (which typically requires higher power) and medical imaging.

To assess the performance of these newly developed materials, high-frequency PIN-PMN-PT single-element transducers at center frequencies of 35 and 60 MHz were designed, fabricated, and tested. An image of a 20-μm-diameter tungsten wire phantom was acquired with the 35-MHz transducer. The measured axial and lateral resolutions were in good agreement with theoretical values.

II. Design and Method

PIN-PMN-PT single crystals were supplied by HC Materials Corps (Bolingbrook, IL). The crystals were grown with a modified Bridgman method [8].The ferroelectric properties which were reported by Tian *et al.* [8] are shown in Fig. 1. The coercive electrical field of ternary PIN–PMN–PT crystals was found to be 6 kV/cm, more than double that of the binary PMN–PT crystal. Thus, a higher electric field or voltage can be applied to the PIN-PMN-PT transducer for ultrasonic imaging. More importantly, the reliability is also improved because the transducers are capable of handling higher voltages. The thermal stability of ternary PIN–PMN–PT crystal is better than the binary PMN–PT. The transition temperature $T_{R/T}$ and Curie temperature T_C of PIN-PMN-PT single crystal, which denote the temperature limits for piezoelectric crystal applications, are increased to 117°C and 160°C. Thus, PIN-PMN-PT transducers can be used at a higher temperature than PMN-PT. Table I gives a comparison of properties for PIN–PMN–PT and PMN–PT.

Two types of PIN-PMN-PT transducers at center frequencies of 35 and 60 MHz were designed with the KLM model-based simulation software PiezoCAD (Sonic Concepts, Woodinville, WA). The size of the piezomaterial was designed to match the standard 50 Ω load of the pulser/receiver electronics. Because of the large difference of the acoustic impedance between the piezomaterial (32.2 MRayl) and the load medium (1.5 MRayl), it was necessary to incorporate acoustic matching layers to enhance the transducer performance. A mixture of Insulcast 501 and Insulcure 9 (American Safety Technologies, Roseland, NJ) and 2- to 3-μm silver particles (Sigma-Aldrich Inc., St. Louis, MO) was selected as the first matching layer (7.3 MRayls), and Parylene (Specialty Coating Systems, Indianapolis, IN) was selected as the second matching layer (2.5 MRayls). In addition, to further improve the bandwidth of the transducers, conductive

epoxy Es-older-3022 (VonRoll Isola, New Haven, CT) (5.9 MRayls) was used as backing material. The simulation results are shown in Fig. 2, where Vi is the exciting voltage and Vo is the response voltage.

The transducers were fabricated following the procedure reported by Cannata *et al.* [9]. The PIN-PMN-PT crystal plate was first lapped down to a thickness of 55 μm for the 35-MHz transducer and 30 μm for the 60-MHz transducer, respectively. The acoustic stack which includes the first matching layer, piezo-material and backing was then diced to 0.6 × 0.6 mm^2 for the 35-MHz transducer and 0.4 × 0.4 mm^2 for the 55-MHz transducer. The active element, which includes first matching, piezo-material, and backing, was then diced to 0.6 × 0.6 mm^2 and 0.4 × 0.4 mm^2, respectively, and insulated with an epoxy (Epotek 301, Epoxy Technology Inc., Billerica, MA) within brass tubes. An additional chrome/gold electrode was sputtered across the silver matching layer and the housing to form the ground connection. Finally, Parylene was evaporated onto the front surface as the second matching layer. An SMA connector was mounted last. After fabrication, the transducer was poled in air at a room temperature under an electric field of 20 kV/cm for about 5 min.

III. Results and Discussion

To evaluate the transducer performance, a series of measurements was performed. The electrical impedance of the transducers was measured in air with an impedance analyzer (Model 4292, Agilent Technologies Inc., Philadelphia, PA). Fig. 3 and Fig. 4 show the electrical impedance magnitude and phase of the 35-MHz and 60-MHz PIN-PMN-PT transducers. The electromechanical coupling coefficient k_t can be determined according to the IEEE standard [10]. k_t was calculated to be 0.56 for the 35-MHz transducer (Fig. 3). At the resonant frequency, the electrical impedance was 80 Ω; the negative phase (–35°) showed the capacitive nature of the device. k_t was calculated to be 0.55 for the 60-MHz transducer (Fig. 4), and the electrical impedance and phase were 75 Ω and –45°, respectively, at the resonant frequency.

Next, the same pulse-echo method and the same loss compensation method reported by Zhou *et al.* [11] and Snook *et al.* [12] were employed to measure the center frequency, bandwidth, and insertion loss of the transducers. In these experiments, degassed water at room temperature was used as the propagation medium. A flat quartz block was placed at a distance of about 1.5 mm in front of the transducer as a target. Panametrics model 5910PR pulser-receiver (Olympus NDT, Waltham, MA) and a LeCroy LC534 oscilloscope (LeCroy Corp., Chestnut Ridge, NY) set at 50 Ω coupling were used as the signal sources and the signal display for measurements, respectively. The pulse–echo responses and spectra of the transducers are plotted in Figs. 5 and 6. The 35-MHz and 60-MHz transducers, respectively, had −6 dB fractional bandwidths of 48% and 47%. The measured bandwidths were slightly lower than those predicted by the model. This discrepancy was most likely caused by either thickness variability in the matching layers or a degradation of the piezoelectric properties of the crystal during fabrication processing. In the measurement of insertion loss, a burst was produced using a Tektronix AFG2020 function generator (Tektronix, Inc., Richardson, TX). The signal loss from the attenuation in water (2.2×10^{-4} dB/mm.MHz^2) and transmission into the quartz target was compensated in the final insertion loss calculation. Insertion loss of the 35-MHz and 60-MHz transducers were calculated to be −15 dB and −17 dB, respectively.

The measured results of the PIN-PMN-PT transducers were summarized and compared with a 45-MHz PMN-PT transducer [11] in Table II. The 45-MHz PMN-PT transducer used the same fabrication procedure as the PIN-PMN-PT transducers except that it was housed in a needle. Both the 35-MHz and the 60-MHz PIN-PMN-PT transducers yielded a bandwidth over 47%, which was slightly higher than that of PMN-PT transducer. The k_t values of PIN-PMN-PT transducers (0.56 and 0.55) were found to be similar to the reported values of the PMN-PT

transducer (0.55). The insertion loss of the 35-MHz PIN-PMN-PT was the same with that of 45-MHz PMN-PT transducer, and the insertion loss of the 60-MHz PIN-PMN-PT was slightly worse. These results reveal that the performances (bandwidth and insertion loss) of the PIN-PMN-PT transducers compares favorably with high-performance PMN-PT transducers.

The wire phantom image was acquired with the 35-MHz PIN-PMN-PT transducer. In this study, the transducer was mechanically scanned by a motor controller DMC-1802 (Galil Motion Control Inc., Mountain View, CA). The Panametrics 5900PR pulser/receiver was used to excite the transducer. The echoes were then digitized by CompuScope-12400 data acquisition card (Gage Applied Technologies, Lockport, IL) at a sampling frequency of 400 MHz and transferred to the PC. The wire phantom consisted of five 20-μm-diameter tungsten wires arranged diagonally with the equal distance in the axial (1.55 mm) and lateral (0.65 mm) directions. The image was acquired as the transducer scanned across the wire phantom placed in degassed water. Fig. 7 shows the image generated using the 35-MHz transducer with the dynamic range of 40 dB. The echo in the red circle was analyzed; the result indicated a lateral resolution of 256 μm at −6 dB and an axial resolution of 55 μm at −6 dB, which were in good agreement with the theoretical values (lateral resolution of 220 μm and axial resolution of 46 μm).

IV. Conclusions

PIN-PMN-PT high-frequency ultrasonic transducers at center frequencies of 35-MHz and 60-MHz have been successfully fabricated. The measured results were in agreement with PiezoCAD simulations. The k_t, bandwidth, and insertion loss of these transducers were similar to those of 45-MHz PMN-PT transducers, and these transducers have improved reliability because of a high T_C and large coercive electric field. Phantom imaging with a 35-MHz transducer was also obtained, which showed an axial resolution and lateral resolution of 55 μm and 256 μm at −6 dB, respectively. These results suggest that the PIN-PMN-PT crystal is a promising candidate for high-frequency medical ultrasonic transducer applications.

Acknowledgments

The authors would like to thank J. Williams for his help in crystal dicing.

This work was partially supported by NIH Grant. No. P41-EB2182 and China Scholar Council (CSC).

References

1. Foster FS, Pavlin CJ, Lockwwod GR, Ruyn LK, Harasiewicz KA, Berude L, Rauth AM. Principles and applications of ultrasound backscatter microscopy. IEEE Trans Ultrason Ferroelectr Freq Control 1993;40(5):608–617. [PubMed: 18263226]
2. Foster FS, Pavlin CJ, Harasiewicz KA, Christopher DA, Turnbull DH. Advances in ultrasound biomicroscopy. Ultrasound Med Biol 2000;26(1):1–27. [PubMed: 10687788]
3. Park SE, Shrout TR. Characteristics of relaxor-based piezoelectric single crystals for ultrasonic transducers. IEEE Trans Ultrason Ferroelectr Freq Control 1997;44(5):1140–1147.
4. Rajan KK, Shanthi M, Chang WS, Jin J, Lim LC. Dielectric and piezoelectric properties of [0 0 1] and [0 1 1]-poled relaxor ferroelectric PZN-PT and PMN-PT single crystals. Sens Actuators A Phys 2007;133(1):110–116.
5. Chen J, Panda R. Review: Commercialization of piezoelectric single crystals for medical imaging applications. Proc IEEE Ultrasonics Symp 2005:235–240.
6. Hosono Y, Yamashita Y, Sakamoto H, Ichinose N. Growth of single crystals of high-Curie-temperature $Pb(In_{1/2}Nb_{1/2})O_3$–$Pb(Mg_{1/3}Nb_{2/3})O_3$–$PbTiO_3$ ternary systems near morphotropic phase boundary. Jpn J Appl Phys 2003;42(1):5681–5686.

7. Karaki T, Nakamoto M, Sumiyoshi Y, Adachi M, Hosono Y, Yamashita Y. Top-seeded solution growth of Pb[($In_{1/2}Nb_{1/2}$),($Mg_{1/3}Nb_{2/3}$),Ti]O_3 single crystals. Jpn J Appl Phys 2003;42(1):6059–6061.

8. Tian J, Han P, Huang X, Pan H, Carroll JF III, Payne DA. Improved stability for piezoelectric crystals grown in the lead indium niobate–lead magnesium niobate–lead titanate system. Appl Phys Lett 2007;91(22):903–905.

9. Cannata JM, Ritter TA, Chen WH, Silverman RH, Shung KK. Design of efficient, broadband single-element (20-80MHz) ultrasound transducers for medical imaging applications. IEEE Trans Ultrason Ferroelectr Freq Control 2003;50(11):1548–1557. [PubMed: 14682638]

10. IEEE. Standard on Piezoelectricity, ANSI/IEEE Std. 1987. p. 176-1987.

11. Zhou QF, Xu XC, Gottlieb EJ, Sun L, Cannata JM, Ameri H, Humayun MS, Han PD, Shung KK. PMN-PT single crystal high-frequency ultrasonic needle transducers for pulsed-wave Doppler application. IEEE Trans Ultrason Ferroelectr Freq Control 2007;54(3):668–675. [PubMed: 17375836]

12. Snook KA, Zhao JZ, Alves CF, Cannata JM, Chen WH, Meyer RJ, Ritter TA, Shung KK. Design, fabrication, and evaluation of high frequency, single element transducers incorporating different materials. IEEE Trans Ultrason Ferroelectr Freq Control 2002;49(2):169–176. [PubMed: 11887795]

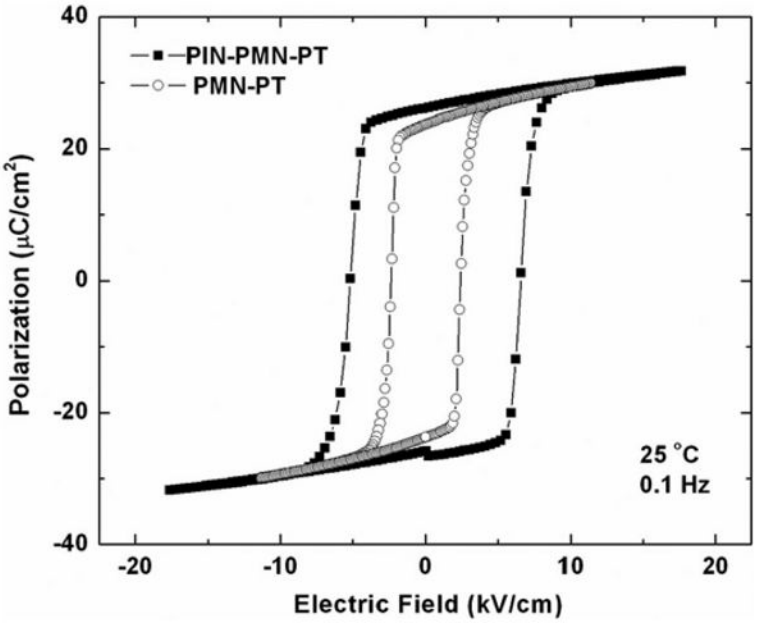

Fig. 1.
Piezoelectric strain and ferroelectric hysteresis for PIN-PMN-PT.

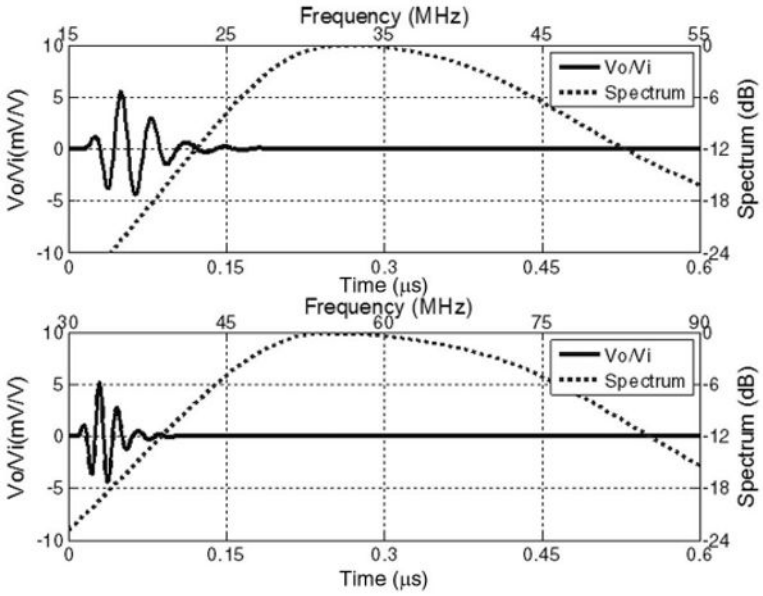

Fig. 2.
Modeled pulse–echo waveform and spectrum for the 35-MHz and 60-MHz PIN-PMN-PT transducers.

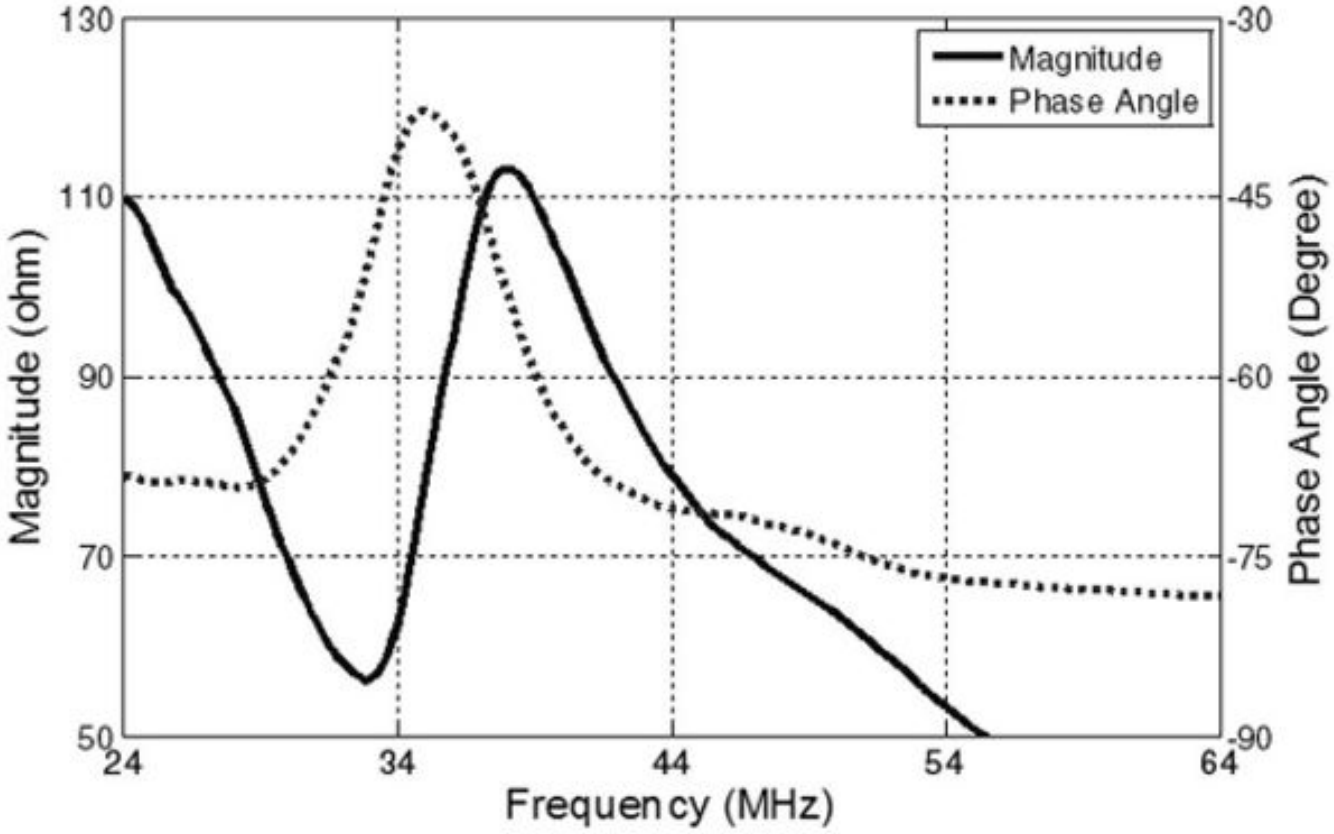

Fig. 3.
Electrical impedance magnitude and phase of the 35-MHz PIN-PMN-PT transducer.

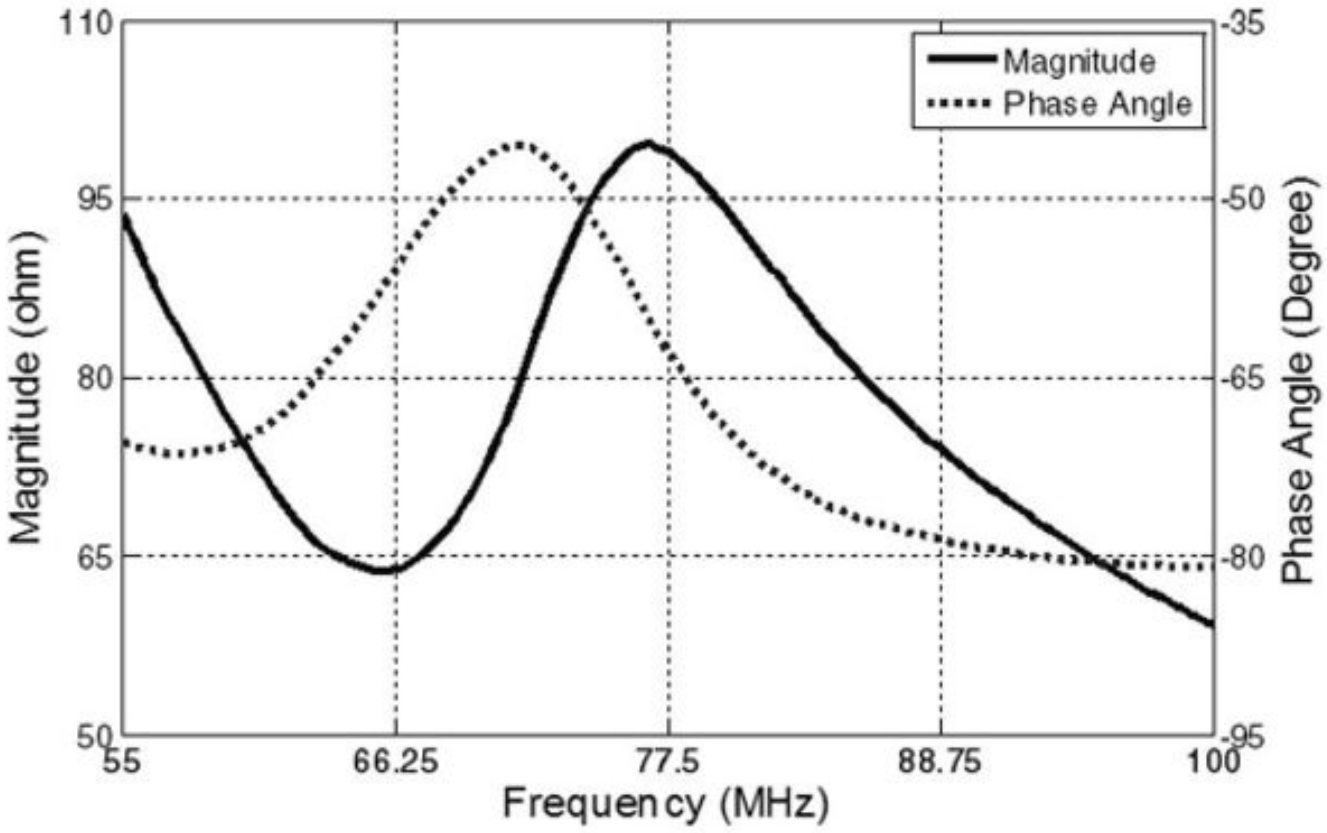

Fig. 4.
Electrical impedance magnitude and phase of the 60-MHz PIN-PMN-PT transducer.

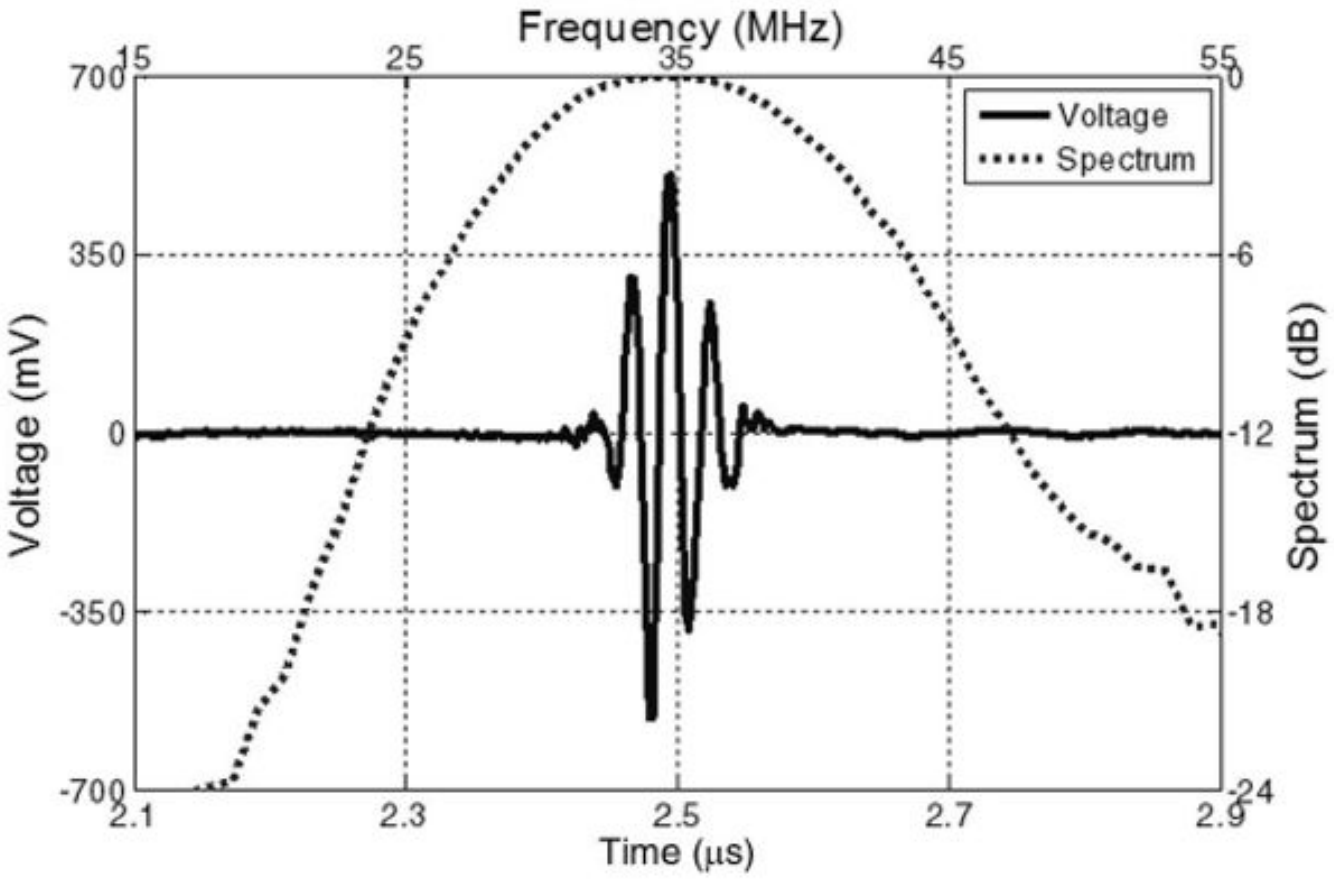

Fig. 5.
Measured pulse–echo waveform and spectrum for the 35-MHz PIN-PMN-PT transducer.

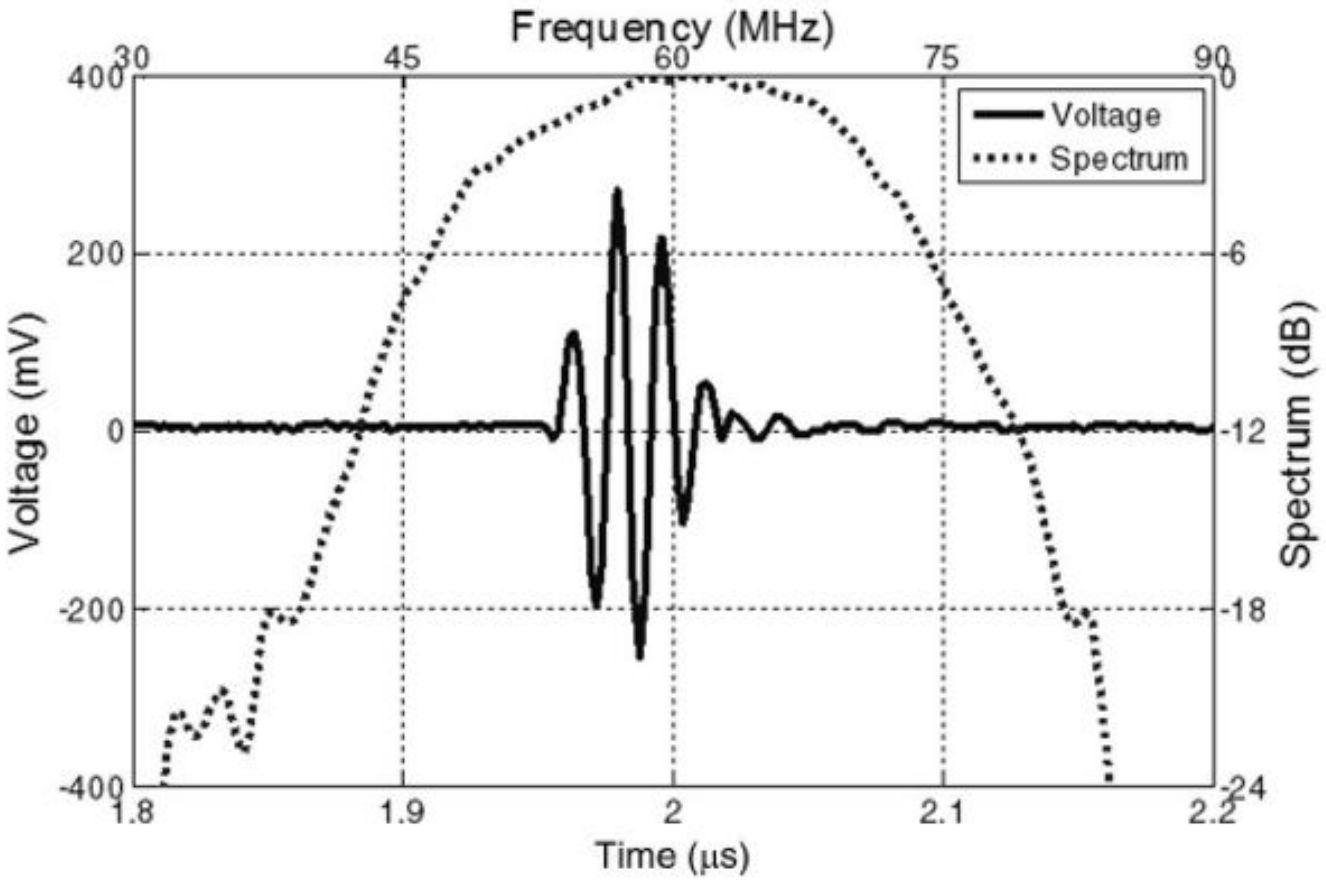

Fig. 6.
Measured pulse–echo waveform and spectrum for the 60-MHz PIN-PMN-PT transducer.

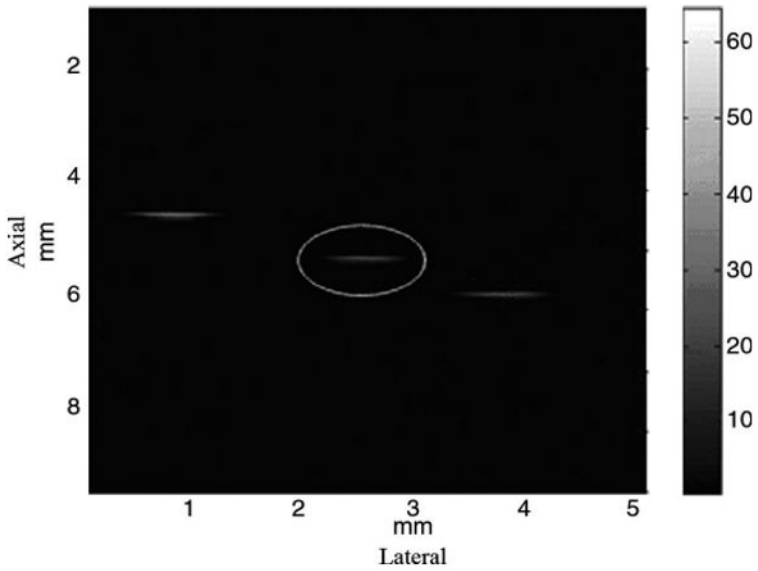

Fig. 7.
Wire phantom image from the 35-MHz PIN-PMN-PT transducer.

Table I

Properties of Piezoelectric Materials

Property	PIN-PMN-PT	PMN- PT [11]
Electromechanical coupling coefficient (k_t)	0.58	0.58
Piezoelectric constant d_{33} of wafer (pC/N)	1301	1430
Relative clamped dielectric constant ($\varepsilon^S/\varepsilon_0$)	700	797
Dielectric loss	0.0036	0.0036
Density (g/cm^3)	8.10	8.00
Longitudinal wave velocity (m/s)	4030	4608
Acoustic impedance (MRayl)	32.6	36.9
Coercivity (kV/cm)	6	2.5
Transition temperature $T_R/_T$ (°c)	117	96
Curie temperature T_C (°C)	160	131

Table II

Modeling and Measured Results for Single-Crystal Transducers

	Modeling results		Measured results		
Transducer	**BW (%)**	**IL (dB)**	k_t	**BW (%)**	**IL (dB)**
35-MHz PIN-PMN-PT	52	−7.5	0.56	48	−15
60-MHz PIN-PMN-PT	53	−9.5	0.55	47	−17
45-MHz PMN-PT [11]	48	−9	0.55	45	−15